# A Smart Sensing Unit for Vibration Measurement and Monitoring

Wilson Wang, *Senior Member, IEEE*, and Ofelia Antonia Jianu, *Student Member, IEEE*

***Abstract*—A novel smart sensing unit is developed in this paper for vibration measurement and machinery condition monitoring. The microprocessor-based smart sensor can collect 2-D vibrations and conduct signal analysis. When mounted in proximity of a bearing housing (a general case), it can conduct online fault detection in shafts and bearings. A correlation spectrum method is proposed as a digital encoder to recognize shaft rotation speed. A wavelet energy spectrum technique is adopted for bearing fault detection. A novel strategy is suggested to extract representative features and enhance feature characteristics by integrating the resulting wavelet energy functions over different frequency bands. The effectiveness of the developed smart sensor and the related fault detection techniques is verified by experimental tests corresponding to different bearing conditions. Test results show that the developed smart sensing unit is an effective measurement and condition monitoring tool; the wavelet energy spectrum technique is a robust bearing fault detection method, especially for nonstationary feature extraction and analysis.**

***Index Terms*—Bearing fault diagnosis, shaft speed detection, smart sensor, wavelet energy spectrum.**

## I. Introduction

A RELIABLE online machinery condition monitoring system is very useful to a wide array of industries to recognize an incipient machinery defect so as to prevent machinery performance degradation, malfunctions, or even catastrophic failures. An early fault warning can enable the establishment of a predictive maintenance program, which is critical to those machines (e.g., airplanes, power turbines, and chemical engineering facilities) to which an unexpected shutdown would cause serious economic or environmental consequences. Fault detection can be conducted based on information carriers such as the acoustic emission, stress waveform, oil analysis, temperature variation, vibration, etc. However, vibration is the most commonly used information form in industrial applications because of ease of measurement and analysis; vibration analysis will also be used in this study.

A classical fault detection system consists of hardware such as sensors, amplifiers, antialiasing filters, a data acquisition board, and a processing computer; it is not only expensive but also inconvenient for implementation in real industrial applications. As the microprocessors become cheaper and faster in processing, smart sensors have been developed to integrate the related data acquisition hardware (e.g., sensors, amplifiers, filters, and A/D converters) onto electric chips, and if possible, to implement some signal processing techniques (e.g., the fast Fourier transform (FFT) and kurtosis) for data analysis. In this paper, a novel smart sensing unit is developed for vibration measurement and signal analysis. It is an extension to a sensing product the authors developed before, in which the vibration is measured by microelectromechanical systems (MEMS) sensors. This new smart sensor uses integrated circuit piezoelectric (ICP) accelerometers that have wider frequency band (up to 20 kHz compared to 5 kHz in MEMS sensors). It is also less sensitive to temperature than MEMS sensors, which is important since most machinery fault results in temperature increase. On the other hand, since most vibration sensors are mounted in proximity of bearing housings (based on mechanical impedance considerations), bearing fault detection techniques will be implemented for online bearing condition monitoring.

Many signal processing techniques have been proposed in literature for machinery fault diagnosis [1], [2], and the authors' research group has also proposed several approaches for fault detection in gearboxes [3]–[6]. In this smart sensing unit, a new technique is developed and implemented for bearing fault diagnosis.

Rolling element bearings are commonly used in various rotary mechanical and electrical systems. Bearing faults, as a matter of fact, are the most common cause of rotary machinery failures. Several techniques have been proposed in literature for bearing fault detection [1], [7] in the time domain [8], [9], the frequency domain [10], [11], and the time–frequency domain [12], [13], respectively. In time-domain analysis, a bearing fault is diagnosed with the help of some statistical indexes (e.g., rms value, crest factor, or kurtosis); however, most of these monitoring indexes are sensitive to noise and operating conditions. Frequency analysis may be the most fundamental approach for bearing fault detection. Bearing health conditions are assessed by examining the fault-related characteristic frequency components in the spectra [14] or some associated expressions such as bispectrum and cepstrum maps [15], [16]. Frequency-based techniques, however, are unsuitable for the analysis of nonstationary signatures that are usually related to machinery defects. Nonstationary or transient signals can be analyzed using time–frequency domain techniques such as short-time Fourier transform (FT) [17], Wigner–Ville distribution [18], or wavelet transform (WT) [3]. In fault diagnosis, the WT is more

Manuscript received May 21, 2008; revised December 22, 2008. First published April 14, 2009; current version published November 18, 2009. Recommended by Technical Editor M.-Y. Chow. This work was supported in part by Materials and Manufacturing Ontario (Canada) and in part by Mechworks Systems, Inc.

W. Wang is with the Department of Mechanical Engineering, Lakehead University, Thunder Bay, ON P7B 5E1, Canada (e-mail: wilson.wang@lakeheadu.ca).

O. A. Jianu is with the Laboratory of Intelligent Mechatronics Systems (LIMS), Lakehead University, Thunder Bay, ON P7B 5E1, Canada (e-mail: oajianu@lakeheadu.ca).

Color versions of one or more of the figures in this paper are available online at http://ieeexplore.ieee.org.

Digital Object Identifier 10.1109/TMECH.2009.2016956

suitable than either the Wigner–Ville transform that contains some cross terms or the short-time FT that has a limited multiresolution solution. According to signal decomposition paradigms, the WT can be performed by the continuous WT [4], discrete WT [19], [20], wavelet packet analysis [21], and extended WT with postprocessing (i.e., using singularity [22], FT [23], [24], and energy density [5], [25]). Although a wavelet packet map can provide more information, its processing results are usually difficult to explain especially when the bearing operates under different load/speed operating conditions.

It should be stated that in machinery condition monitoring, bearing fault diagnosis is one of the most challenging tasks because a bearing is not a simple mechanical component (e.g., a gear or shaft), but a composite system comprising of inner/outer rings and many rolling elements. Each bearing rotary component generates a specific vibratory signal. The impact signatures generated by a bearing defect are usually nonstationary in nature and weak in magnitude, which are modulated by other rotary components (e.g., gears and shafts). As a result, it is generally difficult to extract characteristic features related to bearing health conditions. Consequently, besides the development of the smart sensor, another objective of this paper is to develop and implement a new technique, wavelet energy spectrum analysis, to provide a more reliable approach for online bearing fault detection.

The remaining of this paper is organized as follows. The developed smart sensor is briefly described in Section II. The proposed bearing fault detection technique is discussed in Section III. The effectiveness of the proposed techniques is verified experimentally in Section IV, and some concluding remarks are summarized in Section V.


Fig. 1. Prototype of the developed smart sensing unit.

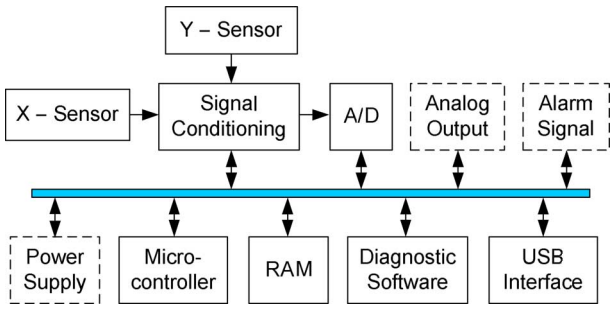


Fig. 2. Block diagram of the developed smart sensing unit.

## II. Description of the Smart Sensing Unit

The developed smart sensor is a microprocessor-based sensing unit, which can collect 2-D vibrations, preprocess the data, and analyze signal properties. When it is mounted in proximity of a bearing housing, it can also conduct online fault detection in bearings and shafts. This smart sensor consists of both hardware and software. The hardware is housed in a rugged enclosure, and a prototype is shown in Fig. 1. Fig. 2 illustrates its main constitute function blocks.

The sensing unit uses two ICP accelerometers (e.g., PCB 320 series) with sensitivity 1.02 mV/($\mathrm{m/s^2}$) and measurement range $\pm 4900\,\mathrm{m/s^2}$ peak. Two sensors are mounted perpendicularly to measure vibrations along $x$- and $y$-direction, respectively.

Signal conditioning functions (e.g., amplification, rectification, and antialiasing filters) are implemented in IC filter chips so as to reduce size and cost. The RAM is a data logger to cache digital data after A/D conversion and the processing results in operations. Fault diagnostic software is implemented for shaft and bearing fault detection. The Universal Serial Bus (USB) interface acts as a serial port to the microcontroller to communicate data in real time with other sources (e.g., a laptop computer). The optional blocks include the analog output, power supply (battery) for stand-alone applications, and the alarm system (in sound or light) to notify health conditions of the machinery system to be monitored.

The properties of this smart sensor can be reprogrammed by a computer (e.g., a laptop) via the USB link, with the help of a special software package. The reconfigurable parameters include sensor ranges, sampling frequency, measuring ranges, filter specifications, time delay, monitoring alarm thresholds, etc.

The implemented software includes general signal analysis algorithms such as the FFT, kurtosis, different digital filters, as well as some available and developed techniques for following fault detection.

1) *Shaft unbalance*: It is based on characteristics such as high spectral amplitude related to shaft speed (but with fewer harmonics), phase relationship (around 90°) between the two sensors, and the dependence on shaft speed.
2) *Misalignment*: It is based on characteristics such as high spectral amplitude related to the second harmonic of the shaft speed (with many higher order harmonics) and high axial vibration responses.
3) *Bearing fault detection*: It is based on kurtosis analysis, spectral analysis, as well as the proposed wavelet energy spectrum analysis discussed in the following section.

## III. New Technique for Bearing Fault Detection

### A. Shaft Speed Detection

Shaft rotation speed $f_r$ is the fundamental parameter not only for fault diagnosis but also for modeling and control applications. If the shaft speed input cannot be provided in applications, a reliable "digital encoder" is very useful to estimate the related shaft speed. On the other hand, even if an approximate speed can be provided in some monitoring applications, accurate speed information from a digital encoder can also be used to improve processing results.

Although shaft speed could be recognized in some spectral maps, the recognized information is not robust but sensitive to noise and operating conditions. In this paper, based on vibrations from two perpendicular directions, a new method is proposed for shaft speed recognition.

Consider two signals $x(t)$ and $y(t)$ along $x$- and $y$-direction, respectively, measured from the smart sensor. The correlation function will be

$$C_{xy}(l) = E\lfloor x(t)y^*(t+l)\rfloor \tag{1}$$

where $E[\cdot]$ is an expectation function and $l$ is the lag index.

The correlation spectrum will be

$$\Phi(f) = R(f)R^*(f) \tag{2}$$

where $R(f) = F[C_{xy}(l)]$, $F[\cdot]$ is the FT function, and $R^*(f)$ is the complex conjugate of $R(f)$.

In analysis, the bandwidth should be at least two times the highest shaft speed of interest, which depends on applications (e.g., 100 Hz in this case).

Shaft speed can then be recognized by examining the resulting spectral map. Fig. 3 shows some examples corresponding to different bearing conditions. The shaft speed ($f_r = 30$ Hz in this case) and its harmonics can be clearly identified from the spectra. Other analytical techniques, such as those illustrated in Section III-B, cannot achieve consistent speed information results.

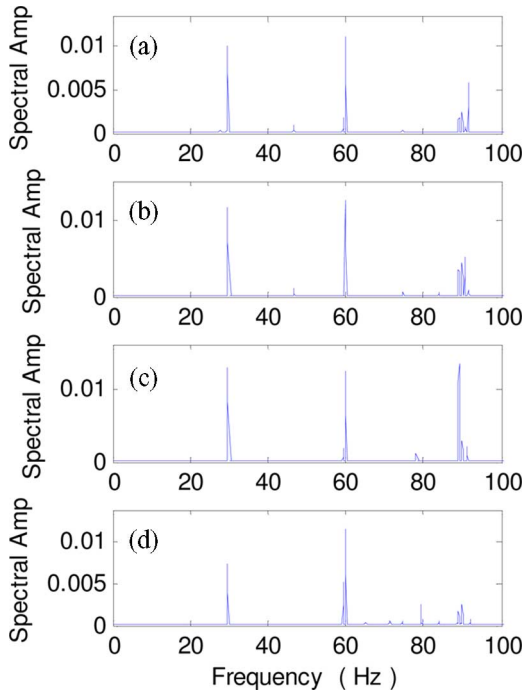


Fig. 3. Examples of shaft speed recognition from (a) a healthy bearing, (b) a bearing with an outer race defect, (c) a bearing with an inner race defect, and (d) a bearing with a rolling element defect.

### B. Bearing Fault Detection Based on Energy Spectrum

A faulty bearing in operation will generate both stationary and nonstationary impacts that excite the bearing and its support structures. The related resonance signatures are usually weak and buried in other high-amplitude vibration signals. The proposed bearing fault detection technique is to recognize these characteristic features. It is an extension from that suggested in [5]: it employs a novel information integration strategy and eliminates the limitations in center frequencies. This technique consists of three procedures: demodulating resonance features by wavelet analysis, integrating the resulting wavelet energy functions to highlight bearing characteristic features, and analyzing correlation spectrum of the synthesized energy function for bearing fault diagnosis.

*1) Determination of Wavelet Energy Functions:* Consider a rolling element bearing with a fixed outer ring (the most common case in applications). Suppose that a defect (e.g., a fatigue pit) has happened on a bearing component. Each time the defect strikes or is struck by another bearing component, an impulse is generated, which excites vibration resonances of the bearing and its surrounding structures. The magnitudes of the impulse transients and the excited resonance modes vary with time. Therefore, it is more suitable to apply the WT for signal analysis.

Consider a time signal $x(t)$, $t = 1, 2, \ldots, n$, where $n$ is the number of samples in the signal; the wavelet functions are determined by

$$T_x(t,s) = \int_{-\infty}^{\infty} x(\tau)\sqrt{s}w^*(-s(t-\tau))d\tau \tag{3}$$

where $w^*(t)$ is the complex conjugation of basic (or mother) wavelet function $w(t)$, and $s$ and $t$ are the respective scale and time variables.

The choice of an appropriate basic wavelet depends on the signal property and the purpose of analysis. In bearing fault detection, the interest is to analyze the resonance features induced by a bearing fault. Therefore, the basic wavelet should possess a similar characteristic as a fault-related transient. By tests, it is found that the Morlet wavelet gives superior results in this application [5]

$$w(t) = \exp\left(-\frac{t^2}{2b_0^2}\right)\exp(j2\pi f_0 t) \tag{4}$$

where $b_0$ is the spread of the wavelet function and $f_0$ is the center frequency that is usually selected as the shaft rotation frequency $f_r$.

To meet admissibility of the WT [26], the following relationship should be satisfied:

$$b_i f_i = \frac{1}{\sqrt{2\ln 2}} \tag{5}$$

where $i = 0, 1, \ldots, m-1$, and $m$ is the number of frequency bands to be considered, and $b_i$ and $f_i$ are the respective spread and center frequency of the $i$th wavelet function.

The WT in (3) will be implemented by

$$T_x(t,s) = \sqrt{s} F^{-1}\left[X(f) W_s(f)\right] \tag{6}$$

where $F^{-1}[\cdot]$ denotes the inverse FT, $X(f)$ is the FT of $x(t)$, and $W_s(f) = b_i\sqrt{2\pi}\exp\left[(-2b_i^2\pi^2(f-f_i)^2\right]$ is the FT of dilated wavelet $w(st)$. The wavelet energy function will be

$$G_x(t,s) = |T_x(t,s)| = \left|\sqrt{s} F^{-1}\left[X(f) W_s(f)\right]\right|. \tag{7}$$

To implement (7) over a designated frequency band, the center frequencies $f_i$ should be properly selected. If the 3-dB bandwidth around $f_i$ is selected for analysis, starting from $f_0 = f_r$, the center frequencies can be determined by

$$f_i = \frac{(1+\alpha)^{i-1}}{(1-\alpha)^i} N f_r, \qquad i = 1, 2, \ldots, m-1 \tag{8}$$

where $N$ is an integer to prevent the influence of shaft-related defects (e.g., misalignment and unbalance), which is $N = 8$ in this case, and $\alpha \approx 0.156$ is a constant determined by 3-dB bandwidth analysis.

The frequency of the analysis is up to $0.5f_s$, where $f_s$ is the sampling frequency. For example, if $f_r = 30$ Hz and $f_s = 20\,000$ Hz, eight frequency bands (i.e., $m = 8$) will be used for signal decomposition with center frequencies of 30, 248, 389, 533, 701, 1001, 1371, 4792 Hz, respectively.

*2) Integration of Wavelet Energy Functions:* In general, bearing-defect-related features will spread over several wavelet frequency bands. Therefore, to enhance feature characteristics and reduce feature size to facilitate real-time monitoring applications, the resulting wavelet energy functions among different frequency bands should be properly integrated. In this paper, the integration is performed by adopting an information entropy function [27].

Suppose $\bar{G}_x(t,s_i) = (1/\sigma_i)G_x(t,s_i)$ is a normalized wavelet energy function, where $\sigma_i$ is the spread of $G_x(t,s_i)$ over the $i$th frequency band; the purpose of normalization is to make $\bar{G}_x(t,s_i)$ independent of scales. The summation is taken by

$$H(t) = \sum_{i=0}^{m-1}\left[K_i \bar{G}_x(t,s_i)\log_\beta \bar{G}_x(t,s_i)\right] \tag{9}$$

where $s_i$ is the $i$th selected scale, and the term $\log_\beta \bar{G}_x(t,s_i)$ is the Harley information of $\bar{G}_x(t,s_i)$, which can be interpreted as the information content of the outcomes $t$ and $s_i$. The logarithm base $\beta = 2$–$8$ is used to scale wavelet coefficient function $\bar{G}_x(t,s_i)$; by simulation, $\beta = 2$ is used in this case. The defined entropy function (9) is the average amount of information contained in random variables $t$ and $s_i$ [27].

In general, fault detection is conducted based on the examination of feature irregularities. Usually, an abrupt change (e.g., increase or decrease) in magnitude and/or phase corresponds to a fault-related feature. Considering that $\bar{G}_x(t,s_i)$ is a normalized $G_x(t,s_i)$ by the spread $\sigma_i$, the signature irregularity over the $i$th band is evaluated with respect to $\beta\sigma_i$, i.e., if $G_x(t,s_i) \gg \beta\sigma_i$, it is believed that there exists some feature irregularity (i.e., some imperfection) that will be highlighted by (9). The synthesis of these wavelet coefficient functions by (9) can integrate the contributions over different frequency bands and enhance the fault feature characteristics.

On the other hand, the amplitude probability density (APD) function is somehow insensitive to many variations of the signal patterns. There is often a "universal" kind of behavior for time histories of variables related to failure: isolated peaks appear first, and then, frequency of appearance increases until the peaks exhibit a more "distributed" character. The sharp peaks affect the tails of the APD function, and the factors sensitive to such pattern variations are of interest in pattern classification operations. Since moments of the APD function are sensitive to changes occurring at its tail, they are possible to be used for faulty feature recognition. Test results have shown that the kurtosis factor is more robust to random functions and signature "outflyers" than other related moments such as the crest factor (the first moment) and skewness factor (the third moment) [8]. Accordingly, the kurtosis factor $K_i$ is used in this study [in (9)] to describe the "peakness" of the APD functions, which is defined as

$$K_i = E\left[\left(\bar{G}_x(t,s_i) - \mu_i\right)^4\right] \tag{10}$$

where $\mu_i$ is the mean of $\bar{G}_x(t,s_i)$ over the $i$th band.

*3) Autocorrelation Spectrum:* The proposed spectrum analysis takes two processes: autocorrelation for the integrated wavelet coefficients $H(t)$ and spectral analysis to enhance the involved periodic features. Specifically,

$$C_{xx}(l) = E\left[H(t)H^*(t+l)\right], \qquad l = 0, 1, 2, \ldots, n-1 \tag{11}$$

where $l$ is the lag index and $H^*(\cdot)$ is the complex conjugate of $H(\cdot)$.

The fault detection is based on spectral analysis (i.e., the FT) of $C_{xx}(l)$ in (11). In implementation, an averaged spectrum over several segments of measured signals (over ten segments in this case) can be used to eliminate some random noise. Bearing health conditions are diagnosed by analyzing the characteristic frequency information on the resulting correlation spectra, as illustrated in the next section.

## IV. Performance Evaluation

The effectiveness of the smart sensor as well as the proposed wavelet energy spectrum technique will be evaluated experimentally in this section.

### A. Experimental Setup

The experimental setup employed in this paper is shown in Fig. 4. The system is driven by a 3-hp induction motor, with the speed ranging from 20 to 4200 r/min. The shaft rotation can be controlled by a speed controller. An optical sensor is used to measure shaft speed. Two ball bearings are fitted in the solid

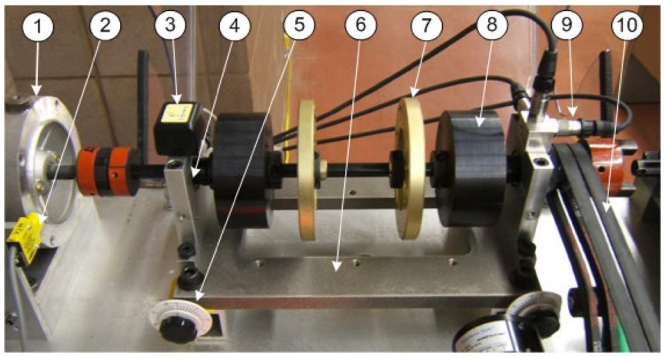


Fig. 4. Experimental setup. (1) Motor. (2) Encoder. (3) Smart sensing unit. (4) Bearing housing. (5) Misalignment controller. (6) Adjustable rig. (7) Unbalance disc. (8) Static load. (9) ICP accelerometers. (10) Dynamic load drive.

housings and tested. The smart sensor is mounted on one of the bearing housings for real-time bearing condition monitoring. To make a comparison, three ICP accelerometers are mounted along three directions on the bearing housings. The dynamic load is applied by a magnetic brake system through a belt drive, and the static load is applied by two heavy disks. The unbalance loads are provided by a pair of thin disks. Misalignment errors can be introduced by an adjustable rig. The signals from the smart sensor are fed to a computer through a USB port. A data acquisition board (NI PCI-4472) is employed for signal collection from the ICP accelerometers and the optical sensor; the board has built-in antialiasing filters with the cutoff frequency set at half of the sampling rate.

### B. Performance Evaluation

Ball bearings (type MB ER-10K) are tested in this paper, with four bearing conditions: healthy bearings, bearings with outer race defects, inner race defects, and rolling element faults. The defect size ranges from 0.2 to 1.6 mm$^2$. Each bearing is tested under different shaft speeds (100–3200 r/min) and load conditions (0.5–2.3 N·m). The tested bearings have fixed outer races. The sampling frequency is 20 000 Hz, and the data size is 100 000 (i.e., over 5 s).

The smart sensing unit provides two vibration signals along $x$- and $y$-direction. As stated in the previous sections, the correlation analysis of these two signals can be used for shaft speed recognition and fault detection in shaft systems such as misalignment and unbalance. In bearing fault detection, the vibration from the $x$-sensor will be used for analysis, whereas another signal from $y$-sensor is employed for two purposes: 1) the processing results can be used to confirm the diagnostic results based on the $x$-sensor so as to improve bearing fault detection reliability and 2) the redundant information can be used for sensor fault detection, such as sensor damage or connection looseness.

To quantify the fault condition of the bearing of interest, a monitoring index $S_\bullet$ is applied to characterize the fault feature properties in the resulting wavelet energy spectrum. The monitoring index $S_\bullet \in [0, 1]$ is defined as the normalized maximum spectral magnitude of the characteristic frequency and its

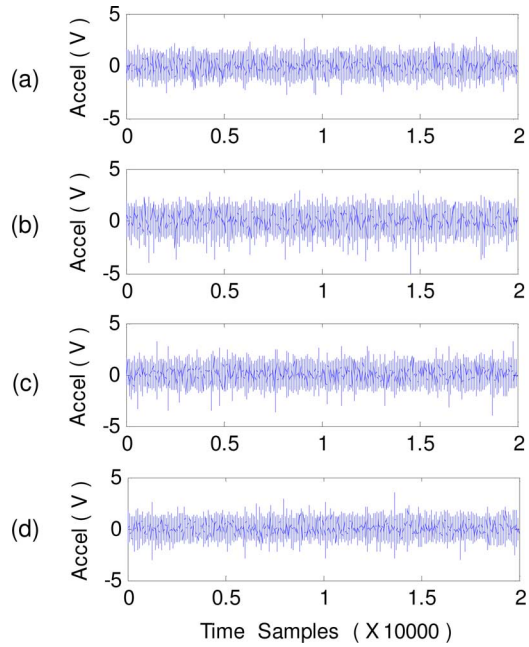


Fig. 5. Part of the measured vibration signals from (a) a healthy bearing, (b) an outer race defect bearing, (c) an inner race defect bearing, and (d) a rolling element damaged bearing.

second and third harmonics. The maximum magnitude is measured by a multibandpass filter, whose center frequencies are the theoretical characteristic frequency and its second and third harmonics. By simulations, the passband of the multipassband filter is selected as $5\% f_r$, where $f_r$ is the shaft rotation speed.

Fig. 5 shows part of the collected vibration signals corresponding to different bearing conditions. It is usually difficult to diagnose bearing health conditions by directly examining original vibration signals. Although Fig. 5(a) contains lower sparks, this indication is not robust for bearing fault detection.

In total, 126 tests have been recorded corresponding to different bearing defect conditions, shaft speed, and load level combinations. Only two defect cases (a small and a medium fault) in each bearing condition, with a shaft speed of 1800 r/min (i.e., $f_r = 30$ Hz) and load of 2.2 N·m, are used to demonstrate the effectiveness of the proposed wavelet energy spectrum. The corresponding bearing characteristic frequencies are $f_{\rm od} = 91.57$ Hz (outer race defect), $f_{\rm id} = 148.43$ Hz (inner race defect), and $f_{\rm ed} = 119.52$ Hz (rolling element defect), which are computed based on the formulas listed in the Appendix. Its performance will be compared with two related techniques: the one-scale WT [24] and the max-envelope method [25].

*1) Healthy Bearings:* Due to the relative motion, bearing components generate vibratory signals in operation. Fig. 6 shows the processing results for a healthy bearing by using the related fault detection techniques. It is seen that the dominant frequency components are related to shaft rotation speed ($f_r = 30$ Hz in this case). Apparently, the spectral map based on the proposed wavelet energy technique provides the highest resolution. The shaft speed indicator can also be recognized on the maps from the max-envelope approach [Fig. 6(b)], even though it has lower resolution due to extra spectral components. The

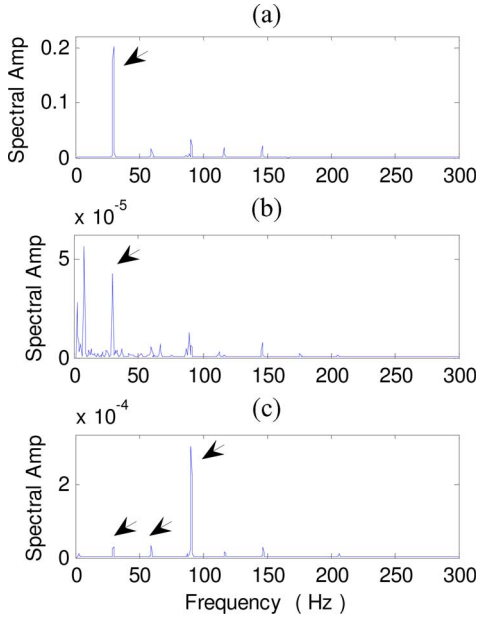


Fig. 6. Healthy bearing processing results using (a) the proposed method, (b) the max-envelope approach, and (c) the one-scale WT. The arrows indicate shaft speed and its harmonics.

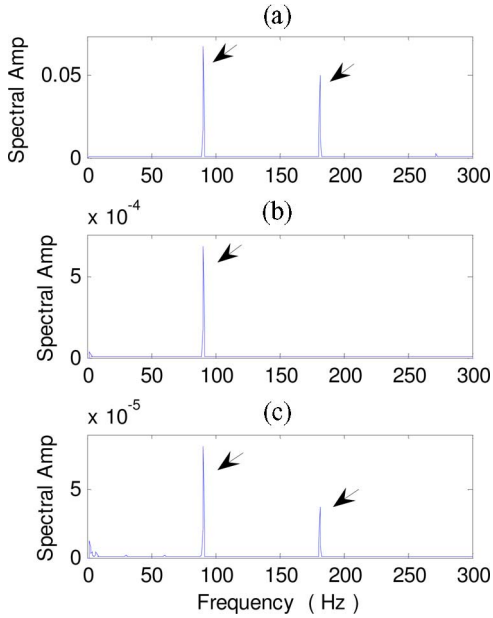


Fig. 7. Outer race fault detection (with a defect about $0.2\ \mathrm{mm}^2$) using (a) the proposed method, (b) the max-envelope approach, and (c) the one-scale WT. The arrows indicate the characteristic frequency and its harmonics.

results from the one-scale WT [Fig. 6(c)], however, may lead to a false diagnosis since the third harmonic of shaft speed (90 Hz) is very close to the outer race defect characteristic frequency ($f_{\mathrm{od}} = 91.57$ Hz). On the other hand, comparing Fig. 3(a) with the processing results in Fig. 6, it is clear that the suggested digital encoder method [in Fig. 3(a)] generates the best speed recognition information.

*2) Outer Race Fault Detection:* In theory, if the bearing is damaged, the corresponding characteristic defect frequency and/or its harmonics could be recognized in its spectra. Figs. 7 and 8 show the processing results for bearings with a small outer race defect (about $0.2\ \mathrm{mm}^2$) and a medium outer race defect (about $0.5\ \mathrm{mm}^2$), respectively. The characteristic frequency is $f_{\mathrm{od}} = 91.57$ Hz. It is seen that each technique can recognize the presence of the bearing fault in this case, because the resonance modes corresponding to a defect on the fixed outer race do not change dramatically in operation. Although both the proposed wavelet spectrum technique and the max-envelope method can provide clear fault detection information, the proposed wavelet energy method generates higher spectral magnitudes because of its feature enhancement effects. In addition, when the defect size becomes larger, the second harmonic of the defect characteristic frequency is highlighted by the one-scale WT [Fig. 8(c)].

On the other hand, shaft speed information cannot be recognized anymore from the spectra in Figs. 7 and 8.

*3) Inner Race Fault Detection:* As stated before, the detection of a fault on an inner race and a rolling element is more challenging than on a fixed outer ring because the modes of the generated impulse resonance features vary with time. Figs. 9 and 10 illustrate the fault detection results corresponding to bearings with a small inner race defect (about $0.2\ \mathrm{mm}^2$) and a medium inner race defect (about $0.5\ \mathrm{mm}^2$), respectively. The characteristic frequency is $f_{\mathrm{id}} = 148.43$ Hz in this case. It is clear that the

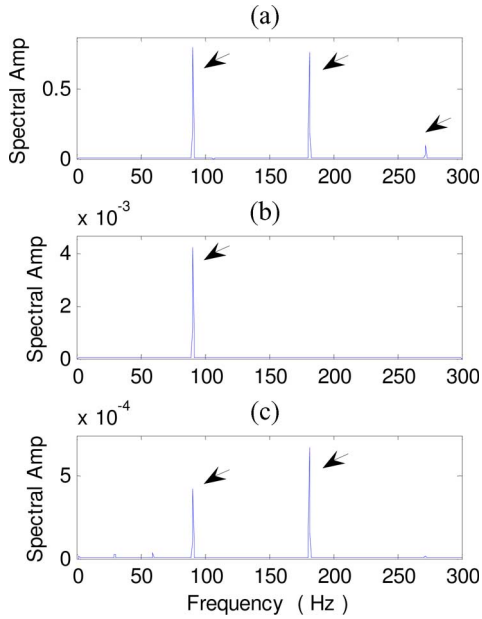


Fig. 8. Outer race fault detection (with a defect about $0.5\ \mathrm{mm}^2$) using (a) the proposed method, (b) the max-envelope approach, and (c) the one-scale WT. The arrows indicate the characteristic frequency and its harmonics.

proposed wavelet energy technique can provide consistent fault diagnostic results; it outperforms another two classical techniques. When the defect becomes larger, the related resonance energy increases, and its monitoring index increases accordingly [from $S_{\mathrm{id}} = 0.89$ in Fig. 9(a) to $S_{\mathrm{id}} = 0.93$ in Fig. 10(a)].

Although the max-envelop method can also detect the bearing defect in this case [$S_{\mathrm{id}} = 0.65$ in Fig. 9(b) and $S_{\mathrm{id}} = 0.71$ in Fig. 10(b)], its spectra contain many extra spectral components that make the fault detection more difficult. In the spectral

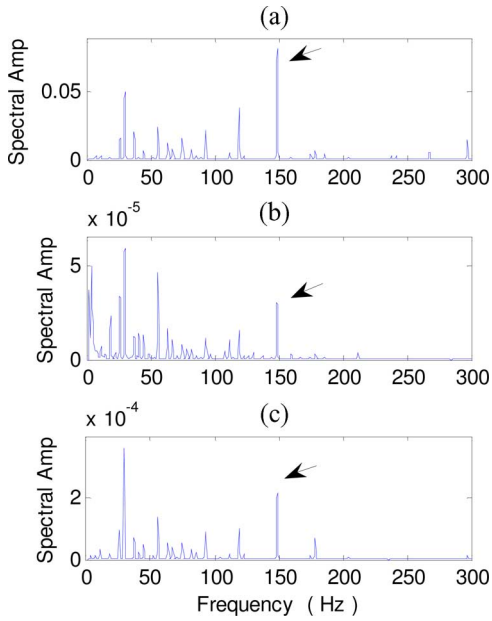


Fig. 9. Inner race fault detection (with a defect about $0.2\ \mathrm{mm}^2$) using (a) the proposed method, (b) the max-envelope approach, and (c) the one-scale WT. The arrows indicate the characteristic frequency.

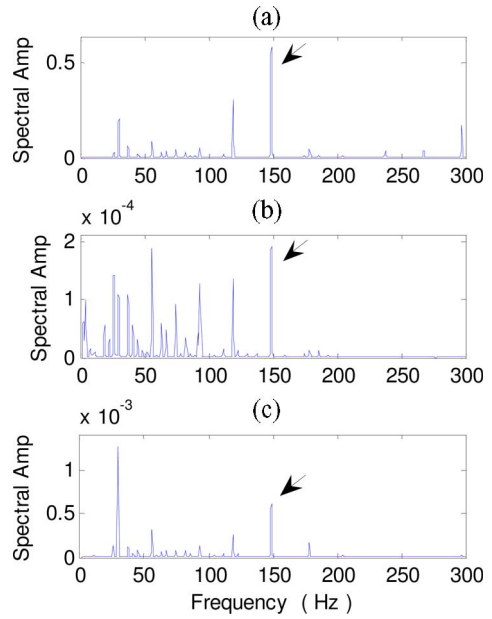


Fig. 10. Inner race fault detection (with a defect about $0.5\ \mathrm{mm}^2$) using (a) the proposed method, (b) the max-envelope approach, and (c) the one-scale WT. The arrows indicate the characteristic frequency.

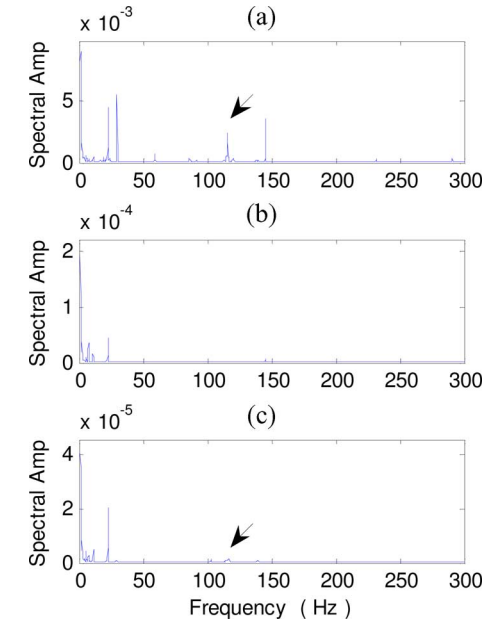


Fig. 11. Rolling element fault detection (with a defect about $0.3\ \mathrm{mm}^2$) using (a) the proposed method, (b) the max-envelope approach, and (c) the one-scale WT. The arrows indicate the characteristic frequency.

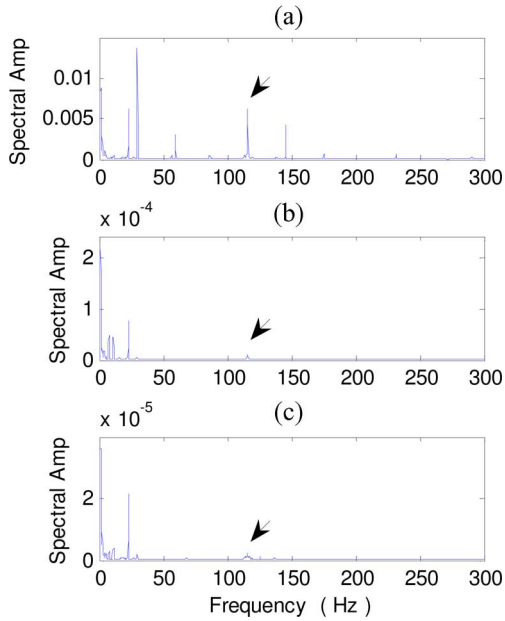


Fig. 12. Rolling element fault detection (with a defect about $0.6\ \mathrm{mm}^2$) using (a) the proposed method, (b) the max-envelope approach, and (c) the one-scale WT. The arrows indicate the characteristic frequency.

maps from the one-scale WT method, the dominant frequency components become the shaft speed, even though the defect characteristic frequency can also be recognized [$S_{\mathrm{id}} = 0.67$ in Fig. 9(c) and $S_{\mathrm{id}} = 0.81$ in Fig. 10(c)]. It should be stated that unclear or confusing processing results may lead to false or missed alarms in real world monitoring applications.

On the other hand, compared with Fig. 3(c), the proposed digital encoder technique outperforms these three methods in this case for shaft speed recognition.

*4) Rolling Element Fault Detection:* Figs. 11 and 12 illustrate the processing results corresponding to bearings with a small rolling element defect (about $0.3\ \mathrm{mm}^2$) and a medium element defect (about $0.6\ \mathrm{mm}^2$), respectively. The representative frequency is $f_{\mathrm{ed}}$ =119.52 Hz in this case. Apparently, both the max-envelop and the one-scale WT techniques cannot recognize the bearing defect and have missed the bearing fault under these test conditions. The proposed wavelet energy spectrum technique is the only method that can detect the existence of

the bearing fault even though the resulting defect characteristic spectral components do not dominate the corresponding spectra. If the defect is small [Fig. 11(a)], the resulting resonant features are very weak ($S_{\rm ed} = 0.59$). As the defect becomes larger [Fig. 12(a)], the impact resonance features become more pronounced, and the characteristic frequency component increases accordingly ($S_{\rm id} = 0.73$).

As a summary, from the aforementioned systematic experimental investigation, it is found that it is usually difficult for classical bearing fault detection techniques to clearly recognize characteristic defect frequencies from nonstationary features such as those generated by bearing defects on the inner races or rolling elements. The proposed wavelet energy spectrum technique can provide consistent fault detection results in these test cases due to its efficient feature enhancement characteristics.

## V. Conclusion

A new type of smart sensing unit was developed in this paper for vibration measurement and machinery condition monitoring. It is a microprocessor-based smart monitor that can collect, preprocess, and analyze vibration signals for fault detection in shafts and bearings. A digital encoder based on correlation spectrum analysis is suggested to automatically recognize shaft speed information. A new signal processing technique (i.e., wavelet energy spectrum) is proposed and implemented for bearing fault detection. Bearing resonance signatures are first demodulated by using wavelet analysis, then the resulting wavelet energy functions are integrated to enhance feature characteristics, and finally, a correlation spectrum is employed to highlight bearing-fault-related feature characteristics. The effectiveness of the smart sensor and the related fault detection techniques has been verified by a series of experimental tests corresponding to different bearing conditions. Test results have demonstrated that the adopted wavelet energy spectrum method is a robust bearing fault detection technique. It outperforms other related classical bearing fault detection methods (e.g., the max-envelop method and one-scale WT technique), especially for nonstationary feature extraction and analysis.

## Appendix

For a bearing with a fixed outer ring and rotating at shaft speed of $f_r$, the characteristic frequencies corresponding to a defect on the inner race ($f_{\rm id}$), a rolling element ($f_{\rm ed}$), and the outer race ($f_{\rm od}$) are as follows:

$$f_{\rm od} = \frac{Zf_r}{2}\left(1 - \frac{d}{D}\cos\theta\right) \tag{A1}$$

$$f_{\rm id} = \frac{Zf_r}{2}\left(1 + \frac{d}{D}\cos\theta\right) \tag{A2}$$

$$f_{\rm ed} = \frac{Df_r}{d}\left(1 - \frac{d^2}{D^2}\cos^2\theta\right) \tag{A3}$$

where $Z$ is the number of rolling elements, $d$ is the rolling element diameter, $D$ is the bearing pitch diameter, and $\theta$ is the contact angle. For bearing MB ER-10K, $Z = 8$, $d = 7.937$ mm, $D = 33.503$ mm, and $\theta = 0$.

## References


[1] J. Korbicz, J. Koscielny, Z. Kowalczuk, and W. Cholewa, *Fault Diagnosis: Models, Artificial Intelligence, Applications*. New York: Springer-Verlag, 2004.

[2] D. Shi and N. Gindy, "Industrial applications of online machining process monitoring system," *IEEE/ASME Trans. Mechatronics*, vol. 12, no. 5, pp. 561–564, Oct. 2007.

[3] W. Wang, "An enhanced diagnostic system for gear system monitoring," *IEEE Trans. Syst., Man, Cybern. B, Cybern.*, vol. 38, no. 1, pp. 102–112, Feb. 2008.

[4] W. Wang, F. Ismail, and F. Golnaraghi, "Assessment of gear damage monitoring techniques using vibration measurements," *Mech. Syst. Signal Process.*, vol. 15, pp. 905–922, 2002.

[5] J. Liu, W. Wang, and F. Golnaraghi, "An extended wavelet spectrum for bearing fault diagnostics," *IEEE Trans. Instrum. Meas*, vol. 52, no. 12, pp. 2801–2812, Dec. 2008.

[6] W. Wang, "An intelligent system for machinery condition monitoring," *IEEE Trans. Fuzzy Syst.*, vol. 16, no. 1, pp. 110–122, Feb. 2008.

[7] I. Onel and M. Benbouzid, "Induction motor bearing failure detection and diagnosis: Park and Concordia transform approaches comparative study," *IEEE/ASME Trans. Mechatronics*, vol. 13, no. 2, pp. 257–262, Apr. 2008.

[8] N. Tandon, "A comparison of some vibration parameters for the condition monitoring of rolling element bearings," *Measurement*, vol. 12, pp. 285–289, 1994.

[9] R. Heng and M. Nor, "Statistical analysis of sound and vibration signals for monitoring rolling element bearing condition," *Appl. Acoust.*, vol. 53, pp. 211–226, 1998.

[10] R. Randall, J. Antoni, and S. Chobsaard, "The relationship between spectral correlation and envelope analysis in the diagnostics of bearing faults and other cyclostationary machine signals," *Mech. Syst. Signal Process.*, vol. 15, pp. 945–962, 2001.

[11] J. Stack, T. Habetler, and R. Harley, "Fault-signature modeling and detection of inner-race bearing faults," *IEEE Trans. Ind. Appl*, vol. 42, no. 1, pp. 61–68, Jan./Feb. 2006.

[12] Q. Du and S. Yang, "Improvement of the EMD method and applications in defect diagnosis of ball bearings," *Meas. Sci. Technol.*, vol. 17, pp. 2355–2361, 2006.

[13] G. Luo, D. Osypiw, and M. Irle, "On-line vibration analysis with fast continuous wavelet algorithm for condition monitoring of bearing," *J. Vib. Control*, vol. 9, pp. 931–947, 2003.

[14] P. Mcfadden and J. Smith, "Vibration monitoring of rolling element bearings by the high-frequency resonance technique-a review," *Tribol. Int.*, vol. 17, pp. 3–10, 1984.

[15] J. Stack, R. Harley, and T. Habetler, "An amplitude modulation detector of fault diagnosis in rolling element bearings," *IEEE Trans. Ind. Electron.*, vol. 51, no. 5, pp. 1097–1102, Oct. 2004.

[16] Y. Choi and Y. Kim, "Fault detection in a ball bearing system using minimum variance cepstrum," *Meas. Sci. Technol.*, vol. 18, pp. 1433–1440, 2007.

[17] T. Kaewkongka, Y. Au, R. Rakowski, and B. Jones, "A comparative study of short time Fourier transform and continuous wavelet transform for bearing condition monitoring," *Int. J. COMADEM*, vol. 6, pp. 41–48, 2003.

[18] B. Kim, S. Lee, M. Lee, J. Ni, J. Song, and C. Lee, "A comparative study on damage detection in speed-up and coast-down process of grinding spindle-typed rotor-bearing system," *J. Mater. Process. Technol.*, vol. 187, pp. 30–36, 2007.

[19] X. Li and X. Yao, "Multi-scale statistical process monitoring in machining," *IEEE Trans. Ind. Electron.*, vol. 52, no. 3, pp. 924–927, Jun. 2005.

[20] I. Cade, P. Keogh, and M. Sahinkaya, "Fault identification in rotor/magnetic bearing systems using discrete time wavelet coefficients," *IEEE/ASME Trans. Mechatronics*, vol. 10, no. 6, pp. 648–657, Dec. 2005.

[21] L. Eren and M. Devaney, "Bearing damage detection via wavelet packet decomposition of the stator current," *IEEE Trans. Instrum. Meas.*, vol. 53, no. 2, pp. 431–436, Apr. 2004.

[22] Q. Sun and Y. Tang, "Singularity analysis using continuous wavelet transform for bearing fault diagnosis," *Mech. Syst. Signal Process.*, vol. 16, pp. 1025–1041, 2002.

[23] C. Wang and R. Gao, "Wavelet transform with spectral post-processing for enhanced feature extraction," *IEEE Trans. Instrum. Meas.*, vol. 52, no. 4, pp. 1296–1301, Aug. 2003.

[24] G. Nikolaou and I. Antoniadis, "Demodulation of vibration signals generated by defects in rolling element bearings using complex shifted Morlet wavelets," *Mech. Syst. Signal Process.*, vol. 16, pp. 677–694, 2002.
[25] J. Cheng, D. Yu, and Y. Yang, "Time-energy density analysis based on wavelet transform," *NDT&E Int.*, vol. 38, pp. 569–572, 2005.
[26] G. Strang and T. Nguyen, *Wavelets and Filter Banks*. Cambridge, MA: Wellesley-Cambridge, 1996, pp. 69–79.
[27] T. Cover and J. Thomas, *Elements of Information Theory*, 2nd ed. Hoboken, NJ: Wiley, 2006.

**Wilson Wang** (M'04–SM'07) received the M.Eng. degree in industrial engineering from the University of Toronto, Toronto, ON, Canada, in 1998, and the Ph.D. degree in mechatronics engineering from the University of Waterloo, Waterloo, ON, in 2002.

From 2002 to 2004, he was a Senior Scientist at Mechworks Systems, Inc. In 2004, he joined Lakehead University, Thunder Bay, ON, where he is currently an Associate Professor in the Department of Mechanical Engineering. His current research interests include mechatronics, signal processing, artificial intelligence, machinery condition monitoring, time-series forecasting, intelligent control, and bioinformatics.

**Ofelia Antonia Jianu** (S'08) received the B.A.Sc. degree in mechanical engineering from Lakehead University, Thunder Bay, ON, Canada, in 2008.

She is currently a Research Associate in the Laboratory of Intelligent Mechatronics Systems, Lakehead University. Her current research interests include signal processing, artificial intelligence, machinery fault diagnostics, and prognostics.